ELSEVIER

www.elsevier.nl/locate/carres

Carbohydrate Research 323 (2000) 111–125

CARBOHYDRATE RESEARCH

N-Linked oligosaccharide structures in the diamine oxidase from porcine kidney

Yunping Huang, Yehia Mechref [1], Milos V. Novotny *

Department of Chemistry, Indiana University, Bloomington, IN 47405, USA

Received 13 January 1999; accepted 30 August 1999

Abstract

Structures of the N-linked glycans released from porcine kidney diamine oxidase (DAO) were characterized utilizing various analytical techniques, including matrix-assisted laser desorption/ionization time-of-flight mass spectrometry (MALDI/TOF-MS), high-performance capillary electrophoresis (HPCE), and high-pH anion-exchange chromatography with pulsed amperometric detection (HPAEC-PAD). The oligosaccharide sequences present in DAO were conclusively determined using specific exoglycosidases in conjunction with MALDI/TOF-MS. The structures found in the glycoprotein are primarily linear, di-, or tribranched fucosylated complex type. MS analysis of the esterified *N*-glycan pool derived from DAO indicated the presence of several di- and trisialylated structures.

Keywords: Exoglycosidases; *N*-Glycan; HPAEC; MALDI/TOF-MS; Porcine kidney diamine oxidase

1. Introduction

The diamine oxidase (DAO) from porcine kidney belongs to the class of proteins designated as copper amine oxidases [EC 1.4.3.6], which contain the copper ion and a tightly bound quinone cofactor [1]. They are homodimers with the subunit sizes ranging typically from 70 to 95 kDa, depending on the enzyme source [2]. In general, the amine oxidases are ubiquitous enzymes that have been detected in bacteria, yeast, fungi, plants, fish, birds, and various mammals. These enzymes catalyze the oxidation of a wide range of biogenic amines (e.g., histamine, mono-, di- and polyamines) to aldehydes, releasing ammonia and hydrogen peroxide. Consequently, they play a key role in the nitrogen metabolism of mammals, plants, and microorganisms [3].

While the catalytic activity [4–6] and inhibitor specificity [7,8] of the porcine kidney DAO have been dealt with extensively, information regarding the structure of this enzyme is largely incomplete. In contrast, the amino acid sequences of some other diamine oxidases such as the enzymes from pea seedlings [9] and *E. coli* [10] have been reported. The structural investigations of the pea-seedling DAO revealed the presence of four potential N-glycosylation sites, two of which were thought to be occupied [2]. Some molecular information on the porcine kidney DAO is still controversial. Obtained through SDS-PAGE, the molecular weight of the native dimeric enzyme was reported to be 170 kDa [11] and 186 kDa [12], respectively, while under reducing conditions, the subunits migrated at 105 kDa [12]. The

* Corresponding author. Tel.: +1-812-855-4532; fax: +1-812-855-8300.

E-mail address: novotny@indiana.edu (M.V. Novotny)

[1] Present address: Department of Chemistry, United Arab Emirates University, PO Box 17551, Al-Ain, UAE.

0008-6215/00/$ - see front matter
PII: S0008-6215(99)00254-2

difference was also evident in the results from these two groups in the reported sequences of the 21 amino acids at the N-terminal. The enzyme has been shown to contain histidyl residues that are essential for its catalytic activity [5]; they serve as the ligand of copper, while the sequence of other amino acids around the enzyme's active site has also been shown [1,13]. The glycoprotein nature of this oxidase has only been established through quantitative sugar analysis and Concanavalin A interaction studies [4]. Total carbohydrate content was determined to be approximately 11%. However, another group claimed that the enzyme had at least 20% carbohydrate content [11].

In this study, we have characterized the structures of *N*-glycans cleaved from the porcine kidney DAO. Following the enzymatic release with *N*-glycanase, the carbohydrate sequence and linkage forms were determined using matrix-assisted laser desorption/ionization mass spectrometry (MALDI/MS) in conjunction with specific exoglycosidases. The monosaccharide sequence and branching information were directly accessible through collision-induced dissociation (CID) mass spectra, while the linkage types were determined using specific enzymes. The monosaccharide composition analysis, carried out through high-pH anion-exchange chromatography (HPAEC) after acid hydrolysis of the N-linked oligosaccharides, provided additional structural information.

2. Results and discussion

A compositional analysis of the oligosaccharide moieties in glycoconjugates often provides important information preceding a more complete structural study of these molecular entities. Monosaccharide composition of the *N*-glycans cleaved from DAO was initially assessed by high-pH anion-exchange chromatography with pulsed amperometric detection (HPAEC-PAD). The *N*-glycan hydrolyzate revealed the presence of fucose, *N*-acetylglucosamine, galactose, and mannose residues, suggesting fucosylated, complex type structures. Moreover, the mole ratios of fucose, *N*-acetylglucosamine, galactose, and mannose were 1.00, 5.52, 2.03, and 5.02, respectively. The mole ratios of fucose to galactose further supported the notion that the majority of the *N*-glycan structures are mostly fucosylated.

A high complexity of the *N*-glycans in DAO was first revealed through an HPAEC-PAD map of the oligosaccharides, with numerous peaks observed (Fig. 1). A comparison between the maps of *N*-glycans cleaved from bovine fetuin (used as a 'standard glycoprotein' in establishing the retention range) and DAO suggested the presence of several neutral, mono-, di-, and trisialylated structures in the DAO glycan pool and a relatively high heterogeneity of these structures (Fig. 1).

The presence of sialylated structures was further supported by obtaining a negative-ion mass spectrum of *N*-glycans cleaved from DAO. The negative-ion mass spectra of acidic oligosaccharides are known to provide valuable information about sialic acids, however, the sensitivities are often much lower than in analyzing neutral sugars in the positive-ion mode. Due to its higher tolerance toward impurities, 6-aza-2-thiothymine (ATT) was used here as the MALDI matrix. The negative-ion mass spectrum of the N-linked oligosaccharide mixture was recorded (Fig. 2). Although ATT is known to be associated with significant fragmentation due to the loss of a carboxyl group from the sialic acid residues [14], the spectrum depicted in Fig. 2 indicates the presence of two sialylated structures corresponding to m/z 2078 and 2370. These m/z

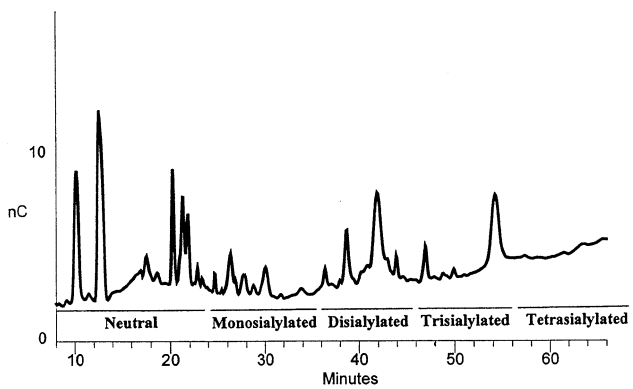

Fig. 1. HPAEC-PAD chromatogram of *N*-glycans of DAO. The horizontal lines indicate the elution time of *N*-glycans of bovine fetuin. Elution program is summarized in Table 1.

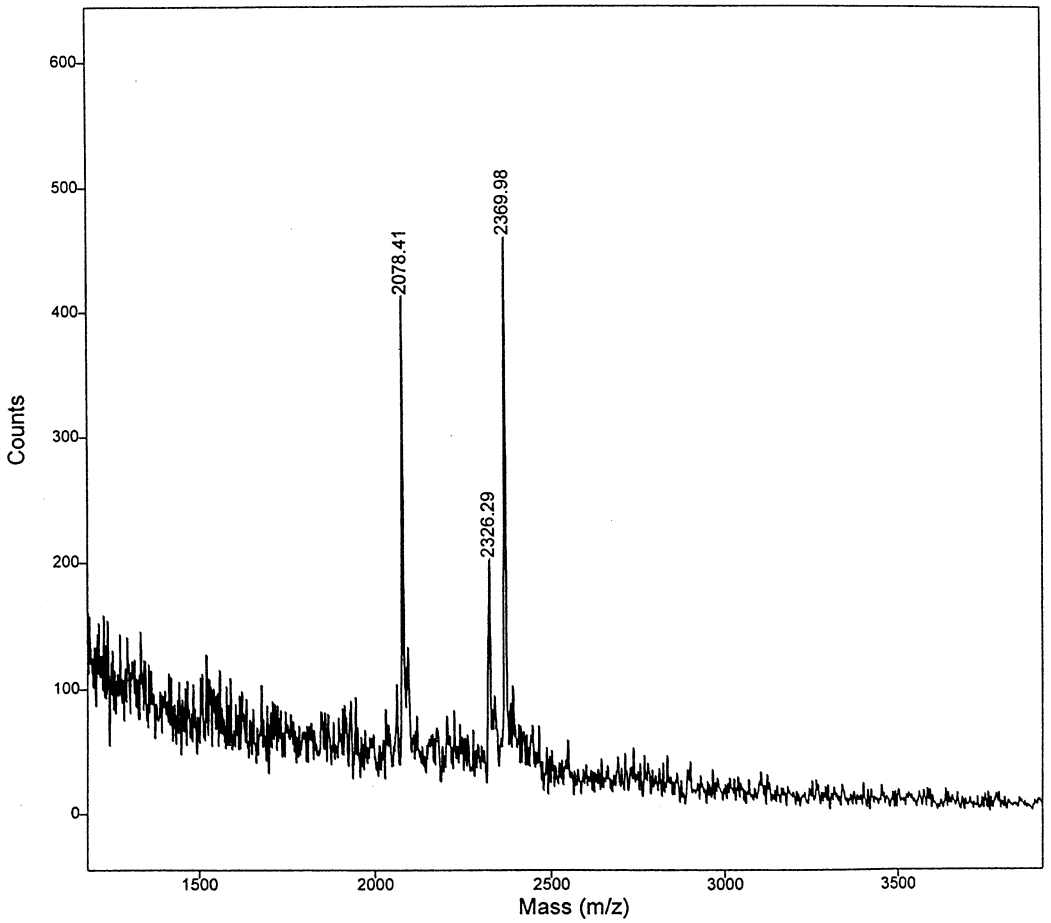

Fig. 2. The negative-ion MALDI/TOF mass spectrum of N-linked acidic oligosaccharides after PNGase F treatment, using ATT as a matrix.

values suggested the presence of mono- (m/z 2078), and disialylated (m/z 2370)/fucosylated biantennary oligosaccharides. The extra signal observed at m/z 2326 was the result of a loss of a carboxyl group from the parent ion at m/z 2370 associated with the use of ATT matrix.

The low sensitivity in the MALDI/TOF-MS analysis of the negatively charged oligosaccharides has generally rendered the technique somewhat ineffective in the analysis of *N*-glycans derived from glycoproteins. However, esterification of the sialic acid residues [16] permits the analysis of a mixture of neutral and acidic oligosaccharides in a single spectrum. This procedure was utilized here to determine a complete mass profile of the *N*-glycan structures present in DAO. The MALDI/TOF mass spectra of the glycans before and after esterification are illustrated in Fig. 3(a) and (b), respectively. As seen from Fig. 3(a), there are several neutral oligosaccharide structures existing in DAO. The four major signals with m/z of 918.1, 1486.52, 1648.87, and 1810.93 were assigned tentative structures in the Figures based on their m/z values and known general structures of *N*-glycans. These structural assignments were corroborated by MALDI/TOF-MS with collision-induced dissociation (CID), one of the commonly used tandem MS techniques, and enzymatic sequencing. Esterification of DAO *N*-glycans allowed the determination of several additional peaks, which had not been seen prior to esterification (compare Fig. 3(a) and (b)); these presumably correspond to the sialylated structures. Tentative structures corresponding to the m/z values observed in Fig. 3(b) are depicted near their respective peaks.

Since the methyl ester of a sialic acid residue has an m/z value of 305, the mass difference between the two m/z values in Fig.

3(a) and (b) suggests the possible existence of one sialic acid residue in the original N-linked oligosaccharides. Similarly, the mass difference of 610 or 1005 indicates the existence of two or three sialic acid residues, respectively. The signals at m/z 2419 and 2114 in Fig. 3(b) were not observed in Fig. 3(a), but they differed from the signal at m/z 1809 (observed in both Fig. 3(a) and (b)) by m/z 305 and 610, respectively. Therefore, it could be concluded that these peaks correspond to mono- and disialylated oligosaccharides originating from the oligosaccharide structure corresponding to m/z 1809 (namely, a complex, fucosylated biantennary structure). These results agree well with the above observations made in the negative-ion mass spectrum.

It appears that the structure corresponding to m/z 3091 is that of a fucosylated, trisialylated triantennary structure. Along the same lines, the signal observed at m/z 2582.64 is believed to be a disialylated structure originating from the structure with an m/z signal at 1969.64 (Fig. 3(b)). However, the corresponding signals were not observed in the negative-ion mass spectrum because of the lower sensitivity of this technique and the overall low concentrations of these oligosaccharides (Fig. 2). While several additional signals were seen upon esterification, some other signals such as m/z 917, 1485, and 1647 were not changed after derivatization. These signals are likely to correspond to neutral structures.

Thus far, the heterogeneity of *N*-glycans of DAO has been demonstrated by HPAEC-PAD and MALDI-MS, while both techniques indicated the presence of several neutral and sialylated structures. The heterogeneity of the neutral structures derived from DAO was further supported by the map obtained through capillary electrophoresis (CE)/laser-induced fluorescence detection for desialylated oligosaccharides (labeled with 8-aminopyrene-1,3,6-trisulfonic acid, trisodium salt (APTS)) (Fig. 4).

Separation in electrophoresis is based on the differential migration velocity of species in an electric field, which is, in turn, dependent on their charge-to-mass ratio. For desialylated *N*-glycans, the separation is more sensitive to differences in structures rather than the charge, since all structures have the same

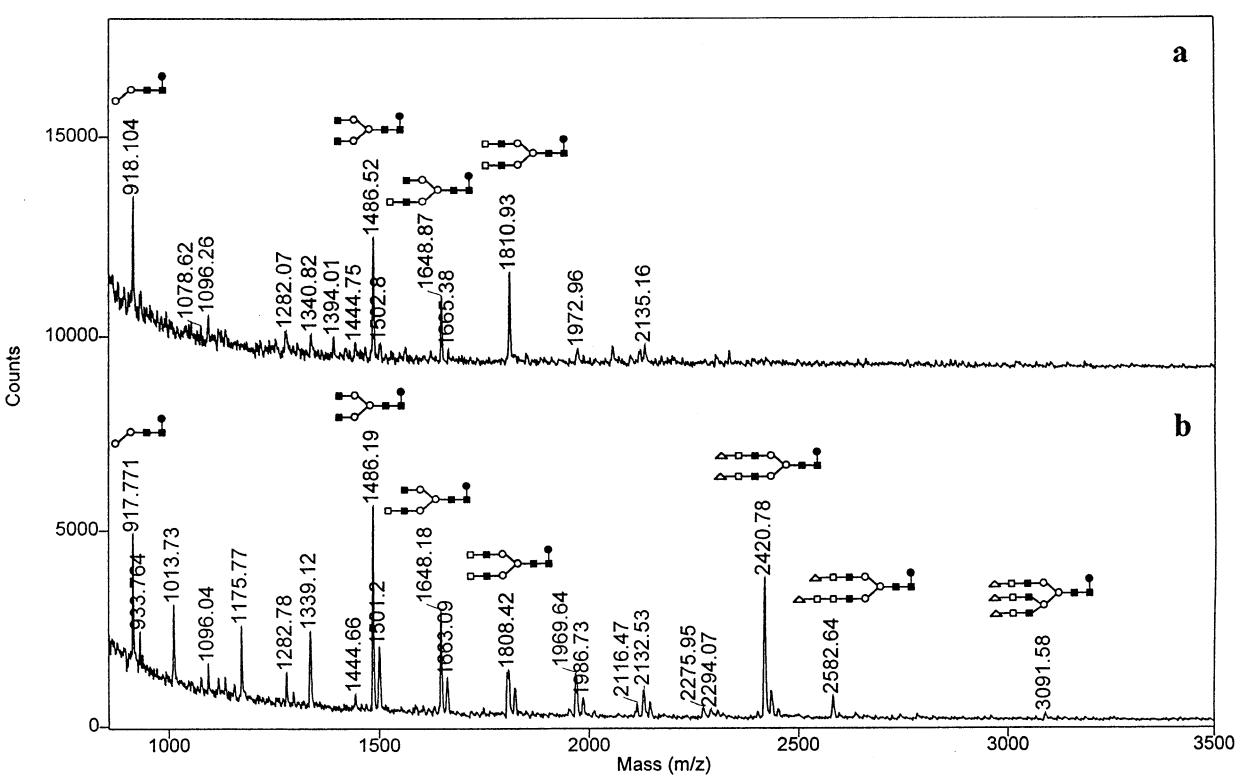

Fig. 3. MALDI/TOF mass spectra of neutral (a) and esterified (b) *N*-glycans derived from DAO. ○, mannose; ■, *N*-acetylglucosamine; □, galactose; ●, fucose; △, methylated sialic acid.

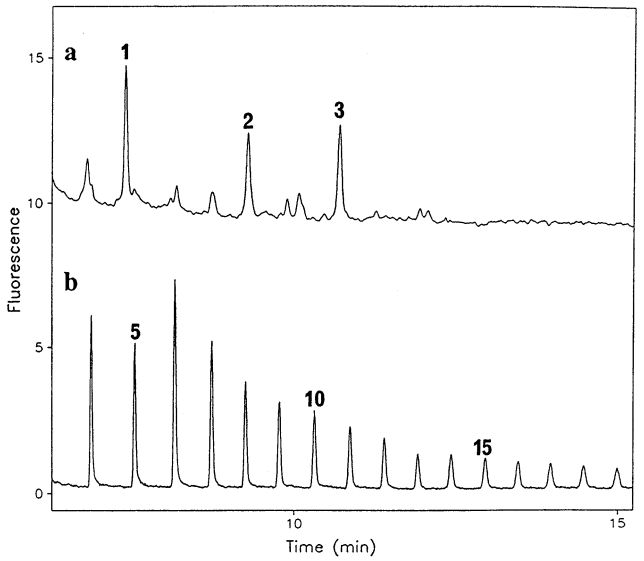

Fig. 4. Electropherogram of APTS-labeled *N*-glycans from the porcine kidney diamine oxidase (a) and APTS-labeled dextrin ladder (b). Capillary column: 37 cm/50 cm × 50 μm i.d. fused-silica column coated with linear polyacrylamide; buffer: 50 mM ammonium acetate (pH 4.5); injection: 10 s (hydrodynamically) at 15 cm height difference; voltage: −15 kV; current: 40 μA.

charge due to the sulfonated APTS label. As a result, the CE map resembles the mass profile obtained by MALDI/MS. The three major peaks (labeled as 1, 2, and 3 in Fig. 4(a)), as observed in the CE map, seem to correspond to the same signals found at *m/z* 917, 1486, and 1809 in the MALDI mass spectrum (Fig. 3(a)). In addition to the three major peaks observed in the CE map, several minor peaks are seen, corresponding to the minor signals appearing in the MALDI mass spectrum (compare Fig. 3(a) and Fig. 4(a)). In order to support this observation, a part of the DAO *N*-glycan pool was loaded onto a size-exclusion chromatographic column, while the fractions were collected and identified by MALDI/MS. The fractions corresponding to *m/z* 917, 1486, and 1809, were labeled with APTS and analyzed by CE. The migration times (data not shown) matched well with the signals shown in Fig. 3(a).

Although most signals in the CE map were accounted for in the MALDI spectrum, an additional peak (migrating faster than the peak corresponding to *m/z* 918) was observed in the CE map, but not in the MALDI spectrum. This additional peak appears to correspond to an *N*-glycan structure with an *m/z* value lower than 800. The inability to observe this signal by MALDI is due to the fact that, in the low *m/z* range, the interference from the matrix becomes substantial, obscuring the analytical results. This problem was overcome through labeling the desialylated DAO *N*-glycans with a neutral reagent, 2-aminobenzamide, thus increasing the observed *m/z* values by 121. The MALDI spectrum of 2-aminobenzamide-labeled *N*-glycans is illustrated in Fig. 5. Labeling of the *N*-glycans thus allowed the determination of an additional structure corresponding to *m/z* 876 (a derivatized structure observed in Fig. 5). The molecular weight of this oligosaccharide is 756, which is 162 Da less than that of the structure with a signal at *m/z* 918 (Fig. 3(a)), indicating the difference of a hexose residue. This labeling strategy could be used as a valuable tool for the determination of low-molecular-weight structures, in general, and alternatively, even more effective mass-expanding reagents could be synthesized for the purpose.

So far, we have demonstrated the heterogeneity of the *N*-glycan pool derived from DAO through the use of HPAEC-PAD, MALDI/TOF-MS and CE. Tentative structures were assigned to the glycans based on their *m/z* values. In order to assess the monosaccharide sequence and branching of the major signals observed in Fig. 3(a) (i.e., *m/z* 917, 1485, and 1809), MALDI/TOF-MS with CID was further utilized. The MALDI/CID MS/MS spectra of the corresponding signals are shown in Fig. 6. Generally, the B- and Y-type fragmentations were commonly observed in the spectra, while the A-type (cross-ring) fragmentation occurred only at the reducing end. With the core structure $(Man)_3(GlcNAc)_2$ present widely in the mammalian glycoproteins [17], the complete oligosaccharide structures due to *m/z* 917, 1485, and 1809 were elucidated through assignment of the fragmentation pathway. The CID spectrum acquired for the signal corresponding to *m/z* 1809 (as observed in Fig. 3(a)) was consistent with a fucosylated biantennary structure (Fig. 6(a)). Moreover, the presence of fragments at *m/z* 1241.06, 1079.07, and 916.4 and the absence of a fragment at

m/z 533 suggested the location of a fucose residue at the reducing-end *N*-acetylglucosamine. The fragmentation pattern observed for m/z 1485 (Fig. 6(b)) was consistent with a fucosylated biantennary structure lacking the two galactose residues at the nonreducing end. The fucose residue was believed to attach to the reducing-end *N*-acetylglucosamine residue, as suggested by the fragment observed at m/z 918. Finally, the fragmentation pattern observed for m/z 917 suggested that this oligosaccharide contains two hexoses, a deoxyhexose, and two *N*-acetylglucosamine residues. A fucose residue was also believed to be attached to the reducing-end *N*-acetylglucosamine. Although the CID-MALDI spectra of the major, neutral *N*-glycans of DAO allowed determination of the monosaccharide sequence and branching, the lack of cross-ring fragmentation hindered a determination of the linkage types. Nevertheless, this information could be obtained through the use of specific exoglycosidases, as seen below.

Based on the m/z values provided from the MALDI/TOF mass spectra alone, we can determine neither the presence of isomeric monosaccharides, nor can we extract the linkage information concerning these monosaccharides. However, the conclusive elucidation of the oligosaccharide structures could be achieved by a sequential digestion with specific exoglycosidases, followed by the

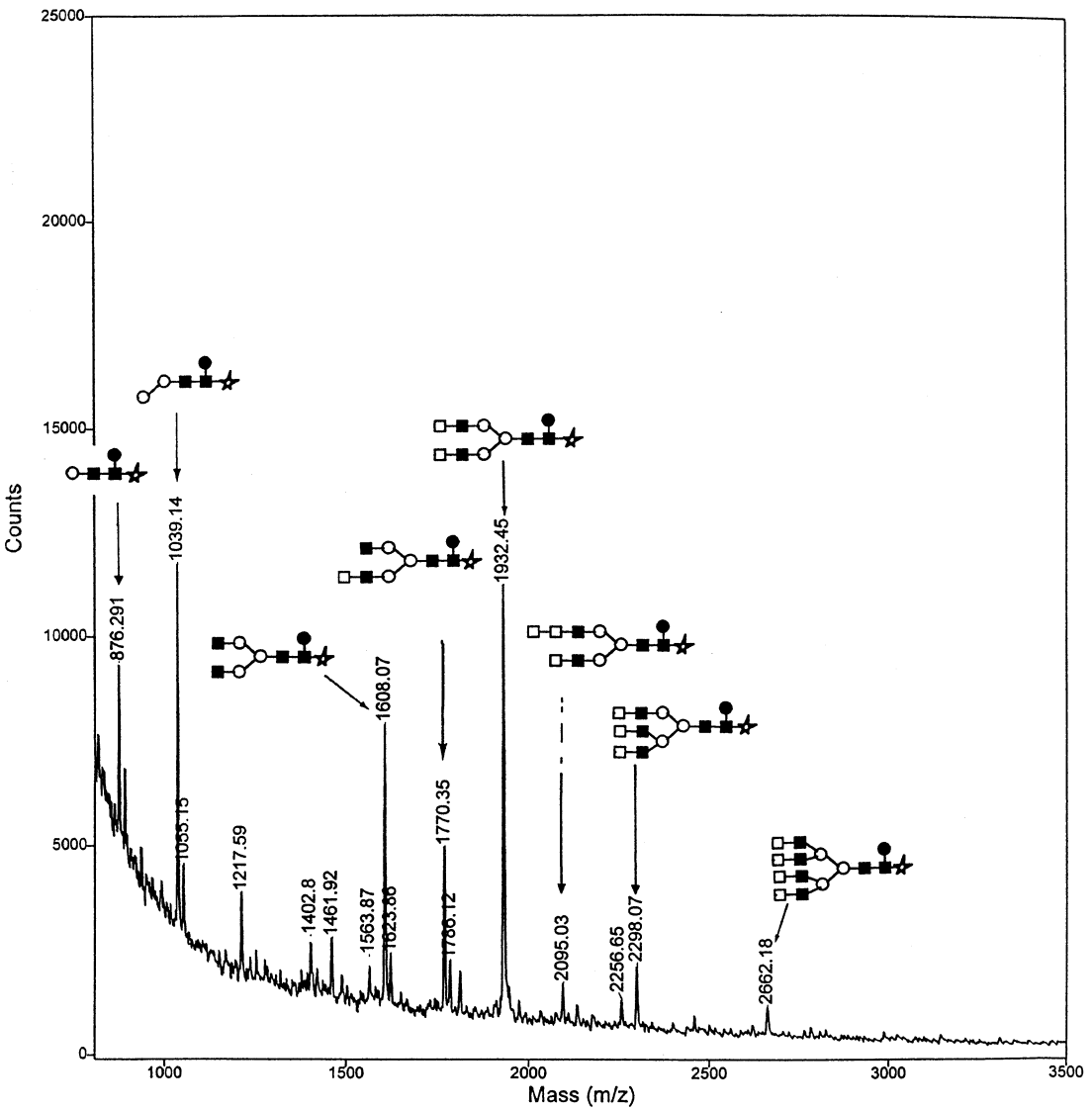

Fig. 5. MALDI/TOF mass spectrum of 2-aminobenzamide-labeled desialylated *N*-glycans from DAO. ○, mannose; ■, *N*-acetylglucosamine; □, galactose; ●, fucose; ☆, 2-aminobenzamide.

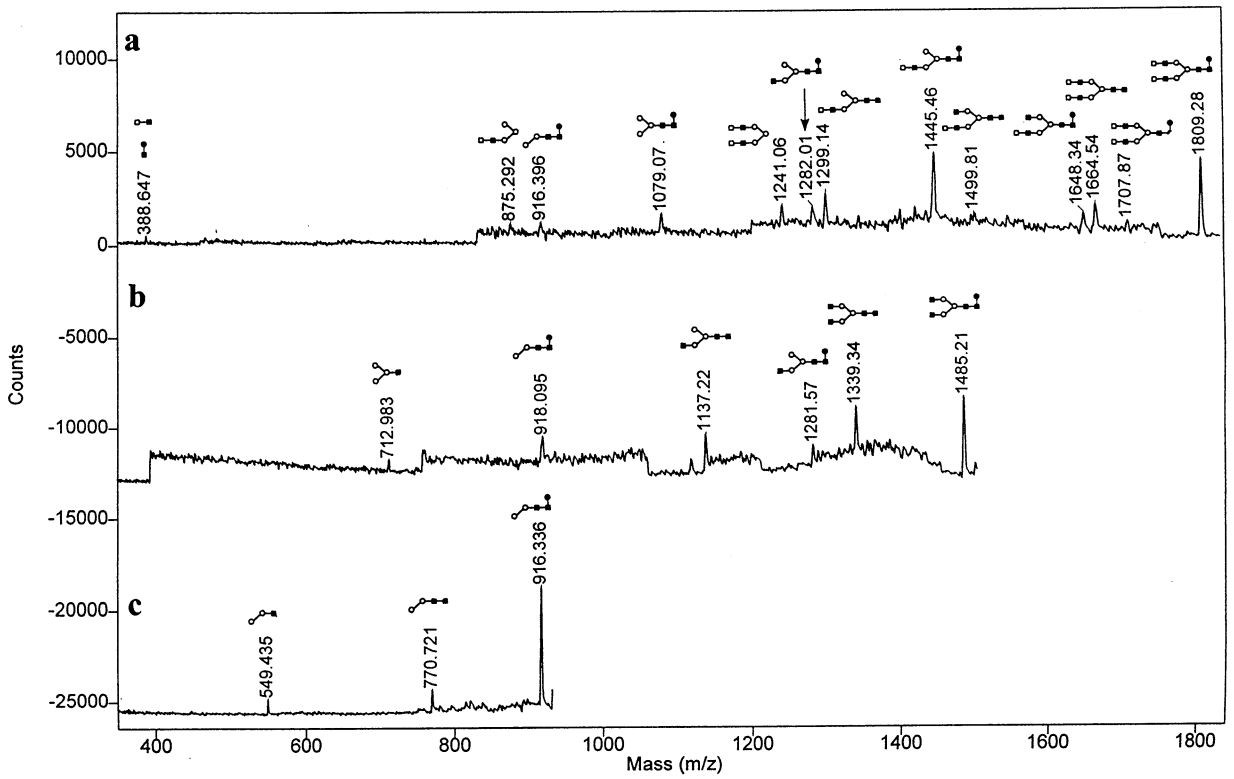

Fig. 6. CID-MALDI/TOF mass spectra of the major components of N-linked oligosaccharides derived from DAO. Precursor ions: m/z 1809 (a), m/z 1485 (b), and m/z 917 (c). Symbols are the same as in Fig. 3.

MALDI/MS analysis of the digest. Several exoglycosidases were thus utilized in order to determine the complete structures of *N*-glycans in DAO.

Several sialylated structures seem to exist in DAO, some of which are mono-, di-, or trisialylated. Therefore, two sialidases with a different specificity were employed in order to determine the linkages of the sialic acid groups. A digestion of *N*-glycans with the sialidase from *Arthrobacter ureafaciens* (specific for α-(2→3/6)) resulted in an increased intensity of the signal at m/z 1809 and the appearance of additional signals that were tentatively assigned as tri- and tetraantennary fucosylated structures (Fig. 7(a)). On the other hand, a treatment of the *N*-glycan pool with the sialidase from Newcastle disease virus (specific for α-(2→3)) resulted in no change in the MALDI spectrum (compare Fig. 7(a) and (b)). The sialic acid linkages of the DAO *N*-glycan structures are thus determined to be exclusively of an α-(2→6) type.

A linkage of the fucose residue to the reducing-end *N*-acetylglucosamine was determined to be of an α-(1→6) type. This result was achieved due to the lack of action by α-(1→3/4)-fucosidase after incubation with the desialylated *N*-glycans (compare Fig. 7(a) and (c)).

The MALDI spectrum obtained after a treatment of the desialylated *N*-glycans with β-galactosidase (specific for β-(1→4) linkage between galactose and *N*-acetylglucosamine) is depicted in Fig. 7(d). The signals at m/z 1809 and 1647 diminished, while the intensity of the signal at m/z 1485 was enhanced upon a treatment with β-galactosidase (Fig. 7(d)). Therefore, the peaks at m/z 1647 and 1809 should correspond to the structures with one and two Gal-β-(1→4)-GlcNAc residues, respectively. Also, the signal at m/z 2173 disappeared while a new signal at m/z 1687 showed, suggesting that the original signal was due to a triantennary structure with three Gal-β-(1→4)-GlcNAc residues. Moreover, the signal at m/z 1443, as observed in Fig. 7(a), disappeared upon the treatment with β-galactosidase, suggesting the presence of a galactose residue on the corresponding structure with a correct linkage.

The signal observed at m/z 1809 (Fig. 7(d)) does not appear to be due to a partial diges-

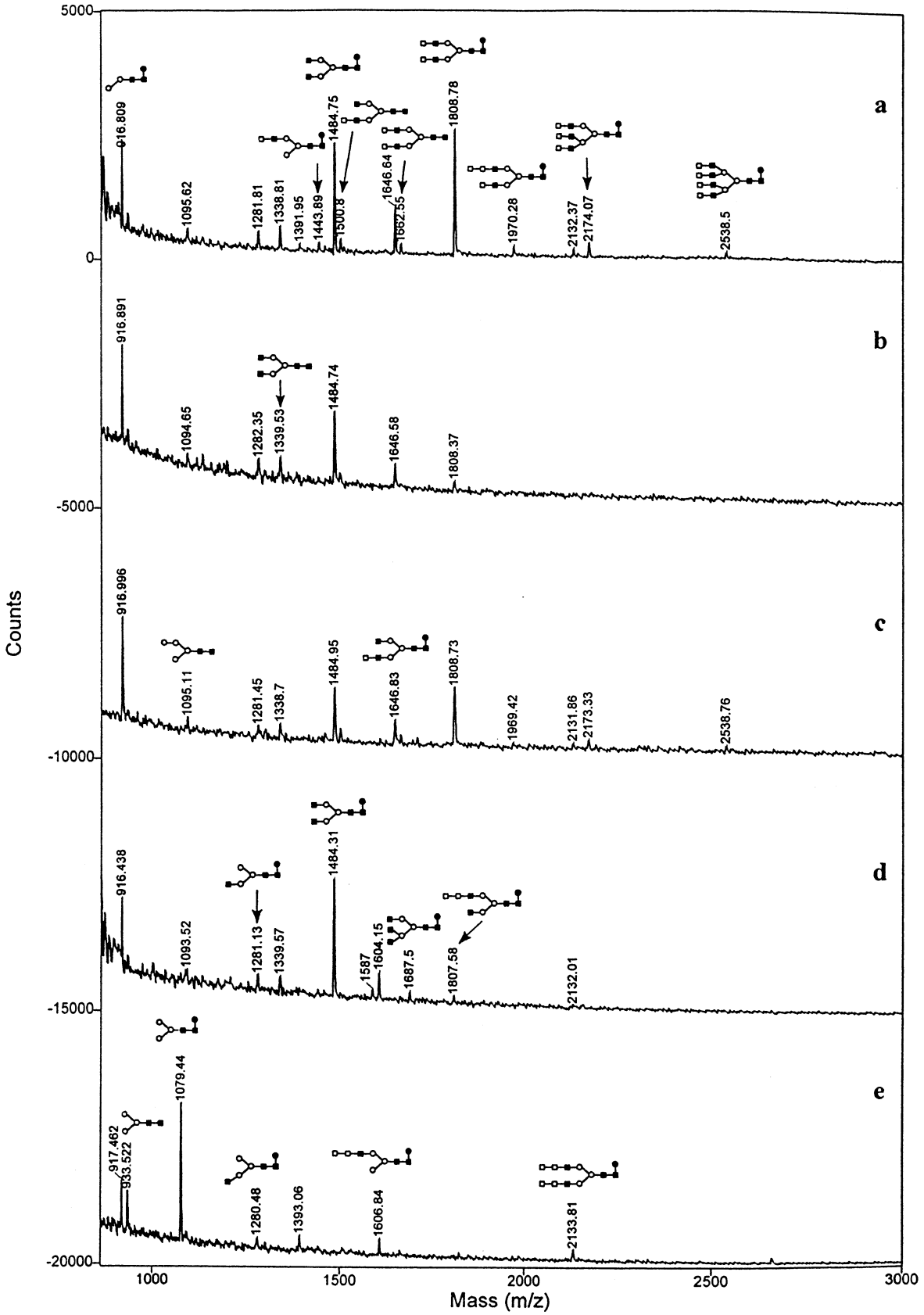

Fig. 7. MALDI/TOF mass spectrum after exoglycosidase digestions: (a) neuraminidase from *A. ureafaciens*; (b) neuraminidase from Newcastle disease virus; (c) neuraminidase from *A. ureafaciens* and α-(1→3/4)-fucosidase; (d) neuraminidase from *A. ureafaciens* and β-galactosidase; (e) neuraminidase from *A. ureafaciens*, β-galactosidase, and *N*-acetylglucosaminidase. Symbols are the same as in Fig. 3.

tion of the corresponding structure (as observed in Fig. 7(a)), but rather from a hydrolysis of one of the galactose residues on the structure corresponding to m/z 1970. The signal at m/z 2132 (Fig. 7(d)) remained unchanged upon the treatment with β-galactosidase, suggesting the presence of a galactose residue on this structure, which is possibly β-(1→3) linked to *N*-acetylglucosamine. Two signals appeared upon incubation with β-galactosidase that could not be structurally assigned.

A successive incubation with *N*-acetyl-β-glucosaminidase caused depletion of the signal at m/z 1485 and appearance of a new signal at m/z 1079 (mass difference of 406), as can be seen in Fig. 7(e). This new signal originated from a loss of two *N*-acetylglucosamine residues, which were α-(1→2) linked to mannose in the structure corresponding to m/z of 1485. The oligosaccharide structure corresponding to m/z 1079 (observed in Fig. 7(e)) is that of a fucosylated mannose core consisting of three mannose residues and two *N*-acetylglucosamine residues. This was further confirmed by a CID spectrum, which is depicted in Fig. 8. In addition, peaks at m/z 1282 and 1339 did not disappear until the N-linked oligosaccharides were treated with *N*-acetyl-β-glucosaminidase, thus suggesting both structures to possess the β-GlcNAc-(1→2)-Man residue. The signal observed at 1606.8 in Fig. 7(e) could originate from the structure corresponding to m/z 1807, as observed in Fig. 7(d), after a loss of an *N*-acetylglucosamine residue. An interesting feature observed in Fig. 7(e) is the emergence of a signal at m/z 933, which corresponds to the mannose core structure. This suggests that the signals observed at m/z values of 933, 1500.8, and 1662.55 in Fig. 7(a) correspond to biantennary structures rather than the potassium adducts of the signals at 916.8, 1484.75, and 1646.64, respectively. A cleavage of the structure corresponding to m/z 1687.5 with *N*-acetyl-β-glucosaminidase (an enzyme specific for β-(1→2) linkages) results in the appearance of a signal at m/z 1280.48, which has a β-GlcNAc-(1→4/6)-Man amenable to digestion by this exoglycosidase.

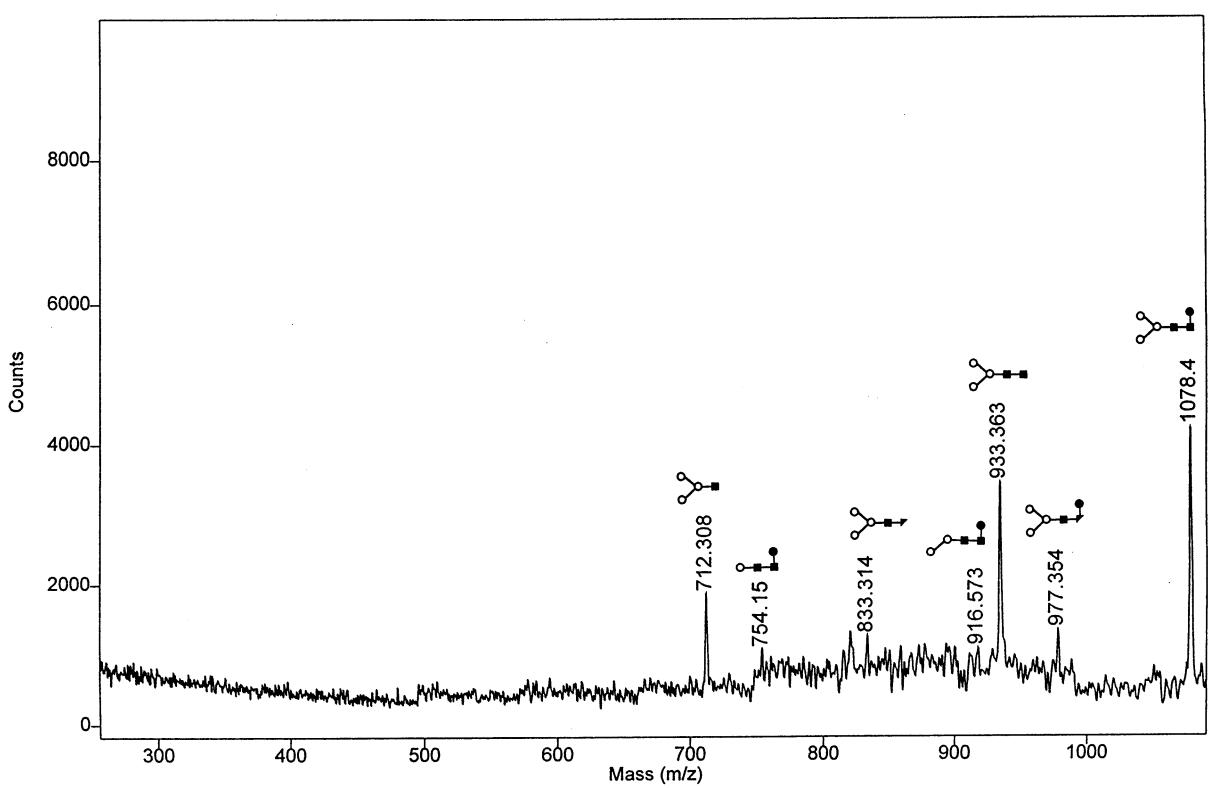

Fig. 8. CID-MALDI/TOF mass spectrum of the fucosylated mannose core structures resulting from the sequential digestion with exoglycosidases, as observable in Fig. 7(e). Symbols are the same as in Fig. 3.

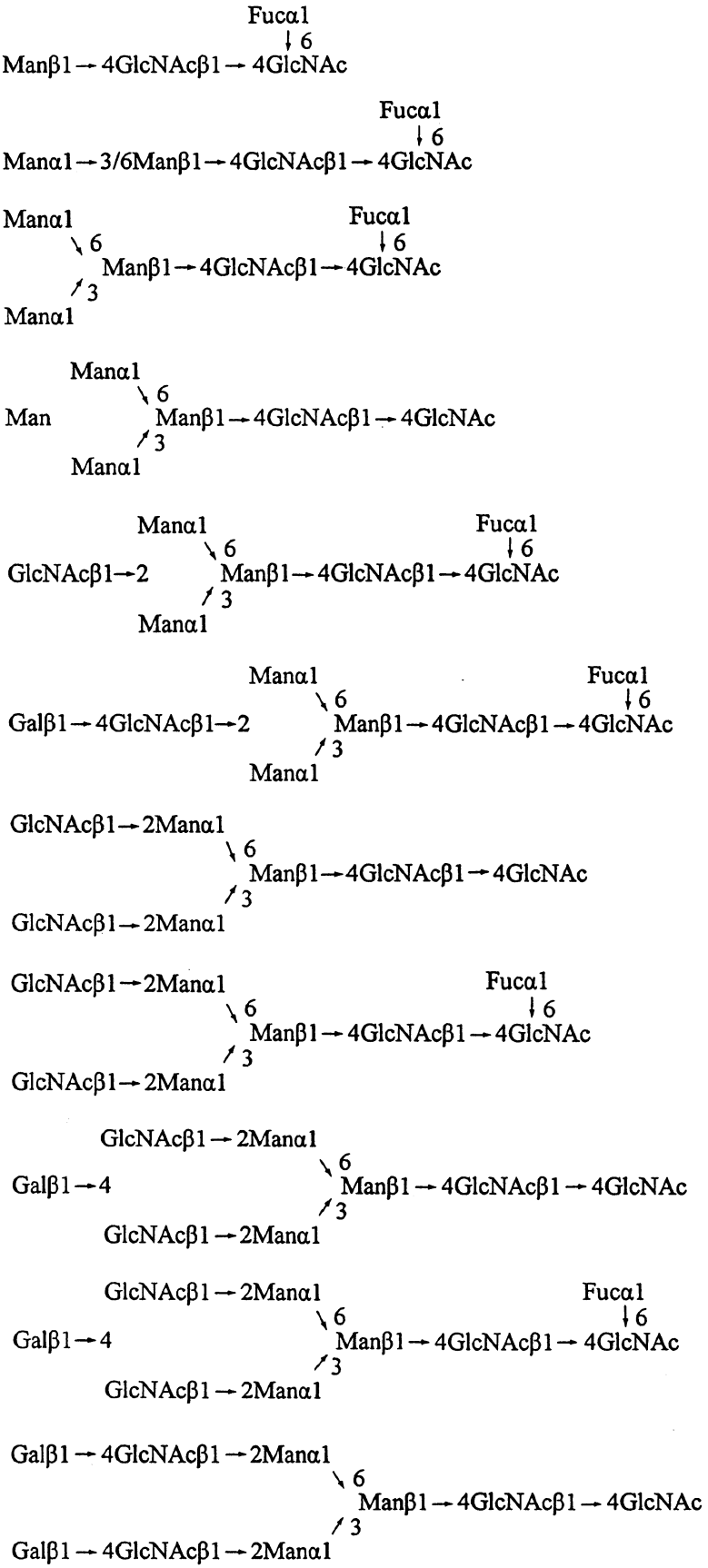

Scheme 1. Structures of the N-linked oligosaccharides of DAO.

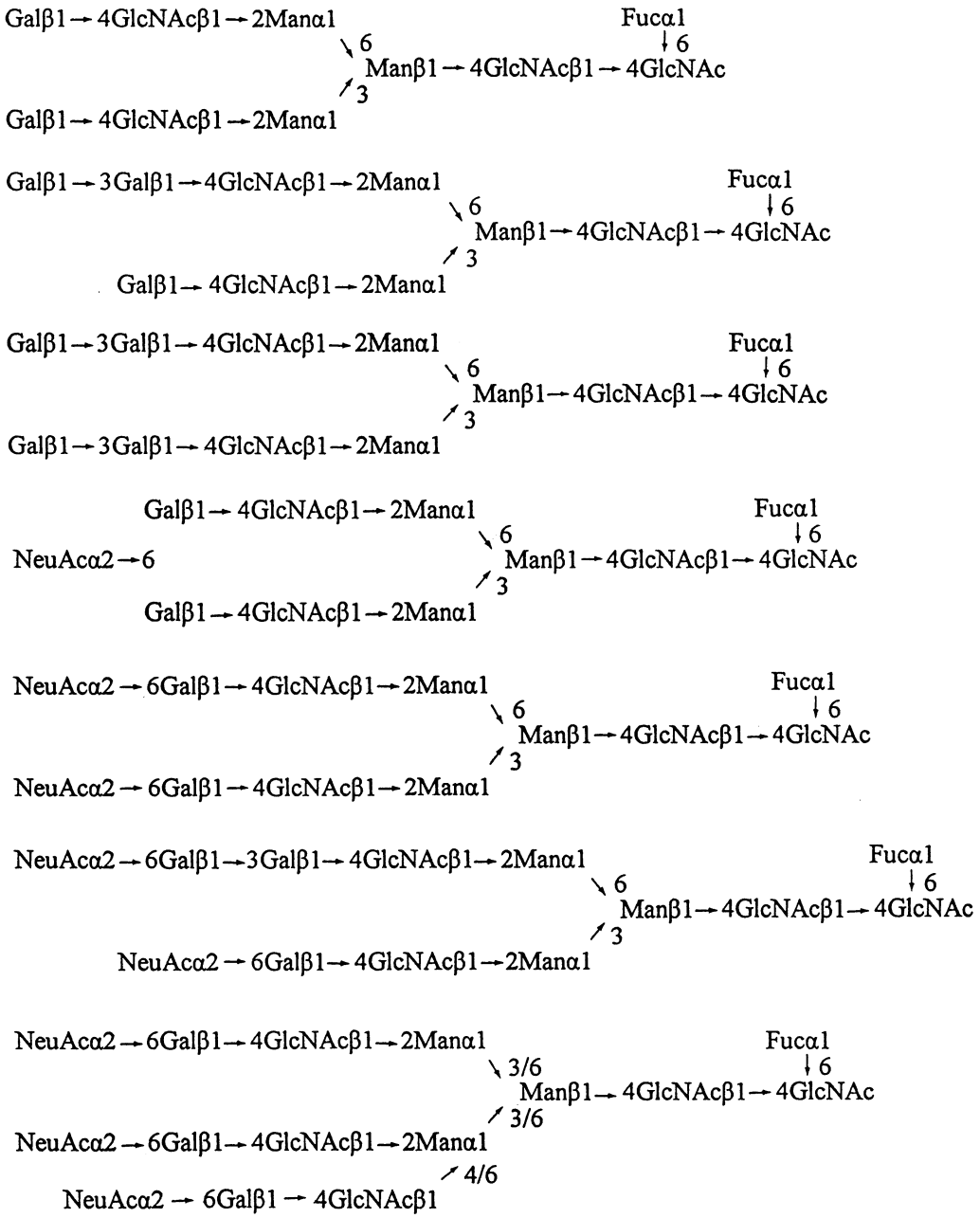

Scheme 1. (*Continued*)

3. Conclusions

A combination of different analytical procedures allowed a comprehensive determination of N-linked oligosaccharide structures in the diamine oxidase enzyme. The structures responsible for an extensive heterogeneity of DAO are illustrated in Scheme 1. The *N*-glycans derived from DAO consist mainly of mono- or disialylated/fucosylated structures. In addition, some minor *N*-glycans exist in DAO, including biantennary and fucosylated/biantennary structures which possess one or two additional galactose residues that are β-(1→3) linked to the nonreducing end (see Scheme 1). Two linear oligosaccharides were also discovered. The high heterogeneity of the oligosaccharides from DAO might be attributed to the presence of several asparagines available for the oligosaccharide linkage. This may also explain the presence of linear structures and incomplete biantennary structures, since the different sites would be competing for the enzymes responsible for building glycan structures.

4. Experimental

Materials.—The porcine kidney diamine oxidase, neuraminidase [EC 3.2.118] from *A. ureafaciens*, dextrin, mannose, glucosamine, galactose, fucose, glucose, 6-aza-thiothymine (ATT), Dowex-50W (H^+), and Dowex 1 (Cl^-) resins were purchased from Sigma Chemical Company (St. Louis, MO). The recombinant enzyme, *N*-glycosidase F (PNGase F), from *E. coli* [EC 3.2.2.18], and exoglycosidases (*N*-acetyl-β-D-glucosaminidase from *Diplococcus pneumoniae* [EC 3.2.1.30], β-galactosidase from *D. pneumoniae* [EC 3.2.1.23], and neuraminidase [EC 3.2.118] from Newcastle disease virus) were received from Boehringer Mannheim Company (Indianapolis, IN). β-(1→3/4)-Fucosidase from *Streptomyces* species [EC 3.2.1.51] was purchased from Glyko (Novato, CA). A fluorescent labeling reagent, 8-aminopyrene-1,3,6-trisulfonic acid, trisodium salt (APTS), was received from Molecular Probes, Inc. (Eugene, OR). Iodomethane was a product of E. Merck (Darmstadt, Germany). Dimethyl sulfoxide, sodium cyanoborohydride, 2-aminobenzamide, and the background electrolytes for capillary electrophoresis (CE) were received from Aldrich (Milwaukee, WI).

Enzymatic cleavage of the N-linked oligosaccharides from DAO.—PNGase F was used to cleave the N-linked oligosaccharides from the glycoprotein. A 5 mg sample of diamine oxidase was reconstituted in 100 μL of 25 mM sodium phosphate buffer solution (pH 7.5), and thermally denatured at 100 °C. Next, 10 μL (two units of activity) of PNGase F solution were added and the solution was incubated for 36 h at 37 °C, during which an additional 10 μL of the enzyme solution was added after 12 h of incubation. A complete cleavage of *N*-glycans from the glycoprotein was evident from SDS-PAGE comparing the undigested and digested samples (data not shown).

N-Glycans were recovered by loading the digests onto a Hi-Pore C_{18} reversed-phase column (RP-304, 250 × 4.6 mm i.d., Bio-Rad Laboratories, Richmond, CA). The chromatographic separation was done using a Series 3B high-performance liquid chromatograph (Perkin–Elmer, Norwalk, CT). The analysis was performed using a 15 min isocratic elution at 10% aq MeCN, followed by a linear gradient elution from 10 to 80% MeCN. The flow rate was set at 1 mL/min. The eluant was monitored by a Linear UVIS-205 (Reno, NV) absorbance detector at 210 nm. The oligosaccharides, which eluted after 6 min, were lyophilized and redissolved in 100 μL of deionized water.

Additional 0.5 μg of DAO protein (1 mg/mL in water) was thermally denatured in a 100 °C water bath for 5 min. After cooling to room temperature (rt), 1 μL of 10 mM phosphate buffer (pH 7.0) and 10 mU of PNGase F were added and the mixture was incubated for 3 h at 37 °C. Subsequently, 1 μL of cation-exchange resin (H^+ form) was added into the digest for a cleanup of sodium ions, while the supernatant was subjected to an MS analysis in the negative-ion mode.

Acidic hydrolysis of N-*glycans.*—Hydrolysis was performed on a 10 μL soln of N-linked oligosaccharides using a standard procedure [15]. The sample was reconstituted into 200 μL of high-purity water and 200 μL of 4 M CF_3COOH in a Teflon-capped, screw-top glass tube. The mixture was heated for 4 h at 100 °C. After hydrolysis, the sample was evaporated to dryness, under a stream of nitrogen, followed by the addition of 20 μL of water and evaporated to dryness again. The procedure was repeated twice to ensure a complete removal of CF_3COOH. The hydrolyzate was redissolved in 100 μL of high-purity water (Stephens Scientific, Riverdale, NJ) and subjected to HPAEC. The calibration curves for the released monosaccharides were established with solutions of the standard monosaccharides at known concentration.

APTS and 2-aminobenzamide labeling of desialylated N-*glycans.*—The dry desialylated sample (from 0.1 mg of DAO) to be derivatized for capillary electrophoresis and the maltose ladder standard were reconstituted separately in 10 μL of 0.1 M APTS or 2-aminobenzamide (prepared in 15% aq AcOH soln) and 10 μL of 1 M aq $NaCNBH_3$. The dissolved mixture was incubated for 2 h at 90 °C. The reaction was stopped by freezing the sample to −20 °C, followed by a drop

dialysis against deionized water for 2 h using 1000 molecular-weight cut-off Spectra/Por membrane (Spectrum, Houston, TX).

Esterification of acidic oligosaccharides.—The sialic acid groups of the acidic N-linked oligosaccharides derived from DAO were esterified according to the procedure described by Powell and Harvey [16]. N-Linked oligosaccharides were applied to a short column (made from a 1 mL plastic syringe) packed with Dowex-50W resin preconditioned with 1.0 M NaOH and deionized water. The eluate was lyophilized and dissolved in 5 μL of dry Me_2SO prior to the addition of 5 μL of MeI. Next, the soln was thoroughly mixed and the esterification was allowed to proceed for 2 h at rt, after which the reaction mixture was dried under a stream of nitrogen, and desalted by passing through a short desalting column made from a 1 mL plastic syringe packed with a mixed Dowex-50W and Dowex 1 resins. The eluate was lyophilized and subjected to MALDI/MS analysis.

Digestion with exoglycosidases.—The N-linked oligosaccharides released from DAO were incubated with specific exoglycosidases to remove their monosaccharides sequentially from the nonreducing end. A MALDI mass spectrum was acquired after each digestion.

To remove the sialic acid residues, the N-linked oligosaccharides released from 2.5 mg of DAO were dissolved in 70 μL sodium phosphate buffer (50 mM), followed by the addition of 12 μL ($\sim$0.12 units of activity) of neuraminidase from *A. ureafaciens*. The mixture was incubated for 18 h at 37 °C.

To remove galactose, 10 μL of the desialylated N-linked oligosaccharide soln ($\sim$25 μg), obtained as described above, was treated with 10 μL ($\sim$10 mUnit) of β-galactosidase from *D. pneumoniae* for 18 h at 37 °C. In order to facilitate its MS analysis, incubation was conducted in the same buffer utilized for the removal of sialic acid residues. Sample aliquots (0.5 μL) were used for the MS analysis.

To avoid a possible interference, β-galactosidase used in the previous step was removed from the mixture by using a 10,000 molecular-weight cut-off micro-concentrator. The galactosidase was retained in the micro-concentrator, while the oligosaccharides were passed. To remove *N*-acetylglucosamine, 2 μL ($\sim$2 mU) of *N*-acetyl-β-D-galactosaminidase soln was added to the 9.5 μL of degalactosylated *N*-glycans. The mixture was incubated for 18 h at 37 °C.

To test the interaction with α-(1→3/4)-fucosidase from *Streptomyces* species, 10 μL ($\sim$10 mU) of α-(1→3/4)-fucosidase soln was added to 10 μL of desialylated N-linked oligosaccharide ($\sim$25 μg) soln. The mixture was incubated for 18 h at 37 °C.

Before treated with neuraminidase from Newcastle disease virus, 5 μL of N-linked oligosaccharide soln was passed through a short column packed with Dowex-50W resin (NH_4^+) to remove the copper ions, which are contained in the amino oxidases and are known as inhibitors of this neuraminidase [18]. The eluate was lyophilized and redissolved in 5 μL of deionized water. Sodium acetate soln (pH 5.5) was added to make the final buffer concentration at 25 mM, and then 5 μL of the enzyme ($\sim$5 mUnit) soln was added. The mixture was incubated for 36 h at 37 °C. Prior to the MS analysis, the mixture was subjected to drop dialysis for 1 h [19].

MALDI/TOF mass spectrometry.—In the positive-ion MS experiments, the matrix used in this study was a recently reported arabinosazone [20]. Samples were prepared for the MALDI/MS analysis by spotting 1.0 μL of sample soln on a polished stainless-steel plate, followed by the addition of 1.0 μL 'arabinosazone' soln (prepared in ethanol at 10 mg/mL concentration). The spots were allowed to dry at rt prior to a mass-spectrometric analysis. In the negative-ion mode, samples were mixed with ATT matrix soln on the MALDI plate. ATT matrix was prepared in 1 mg/mL soln of EtOH and 20 mM ammonium citrate (1:1 v/v), according to a published paper [14].

MALDI mass spectra were acquired on a Voyager-DE™ RP BioSpectrometry Workstation MALDI time-of-flight (TOF) mass spectrometer (PerSeptive Biosystems, Framingham, MA). The instrument uses a pulsed nitrogen laser (337 nm) and can operate in both the linear and reflectron modes. The instrument has the delayed ion extraction capability.

Table 1
Gradient utilized for obtaining HPAEC-PAD maps of sialylated *N*-glycans

Time (min)	Eluent 1 (%) (250 mM NaOH)	Eluent 2 (%) (500 mM NaOAc)	Eluent 3 (%) (deionized water)
0	40	0	60
10	40	0	60
60	40	50	10
70	40	50	10

The ion path is 1.3 m in the linear mode, and 2.0 m in the reflector mode. The acceleration voltage used was 20 kV and the spectra were recorded exclusively in the positive-ion mode. The pressure in the ion source was maintained between 1.0×10^{-7} and 1.0×10^{-6} torr. All acquired spectra were smoothed by applying a 19-point Savitzky–Golay smoothing algorithm [21]. All mass spectra from the positive-ion mode were externally calibrated by a two-point calibration using a dextran ladder (average MW of 8800) standard, while the negative-ion mass spectra were externally calibrated using the known oligosaccharides derived from bovine fetuin. This permitted measurements with a mass accuracy $< 0.1\%$. The low-mass gate was set at 800 Da in order to prevent matrix ions from saturating the detector.

A timed-ion selector was used for the acquisition of CID spectra, selecting the precursor ions. Argon was chosen as the target gas. The acceleration voltage was kept at 20 kV, while the potential values at the reflectron were decreased successively at the rate of 10% by adjusting the mirror ratio, thus allowing the detection of specific fragments at one time. A total of 10–12 segments were acquired at different mirror ratios, while the instrument software combined all segments to generate a CID spectrum.

Capillary electrophoresis.—All electrophoretic separations were performed with a home-made capillary electrophoresis/laser-induced fluorescence (CE/LIF) system described previously [22]. The system consisted of a high-voltage dc power supply (0–40 kV) (Spellman High Voltage Electronics Co., Plainview, NY). On-line fluorescence detection was accomplished using an argon-ion model 543-AP laser (Omnichrome, Chino, CA) (5 mW power at 457 nm). Fluorescence emission at 514 nm was collected through a microscope lens and monitored using a R928 photomultiplier tube (Hamamatsu Photonics K.K., Shizuoka Prefecture, Japan). The signal was amplified with a lock-in amplifier (EG&G Princeton Applied Research, Princeton, NJ).

The separation was conducted in a fused silica capillary (37 cm effective length, 50 cm total length, and 50 μm i.d.), coated with a linear polyacrylamide according to a previously published procedure [22]. The electrophoretic separation was performed using -15 kV, with 50 mM ammonium acetate (pH 4.5) as the background electrolyte. Under these separation conditions, the current generated inside the capillary column was ~ 40 μA. The samples were injected hydrodynamically for 10 s at 15 cm height difference.

Anion-exchange chromatography.—The monosaccharides and sialylated oligosaccharides were separated on a Dionex CarboPac PA-1 anion-exchange column (4×250 mm, Dionex Corp., Sunnyvale, CA) and detected by the model ED40 electrochemical detector in its integrated pulsed-amperometric detection mode. For the monosaccharide analysis, an isocratic elution was performed with a 16 mM NaOH soln at a flow rate of 0.8 mL/min. For the sialylated oligosaccharides, the elution program was utilized, as summarized in Table 1, with the flow rate set at 1.0 mL/min. The chromatograph was computer-controlled, performing the data analysis through the PeakNet software (Dionex).

Acknowledgements

This study was supported by Grant GM24349 from the National Institute of General Medical Sciences, US Department of Health and Human Services.

References

[1] S.M. Janes, M.M. Palcic, C.H. Scaman, A.J. Smith, D.E. Brown, D.M. Dooley, M. Mure, J.P. Klinman, *Biochemistry*, 31 (1992) 12147–12154.
[2] A.J. Tipping, M.J. McPherson, *J. Biol. Chem.*, 270 (1995) 16939–16946.
[3] S.M. Janes, D. Mu, D. Wemmer, A.J. Smith, S. Kaur, D. Maltby, A.L. Burlingame, J.P. Klinman, *Science*, 248 (1990) 981–987.
[4] M.A. Shah, R. Ali, *Biochem. J.*, 253 (1988) 103–107.
[5] M.A. Shah, R. Ali, *Biochem. Mol. Biol. Int.*, 33 (1994) 9–19.
[6] A.A. Coleman, C.H. Scaman, Y.J. Kang, M.M. Palcic, *J. Biol. Chem.*, 266 (1991) 6795–6800.
[7] W.F. Novotny, O. Chassande, M. Baker, M. Lazdunski, P. Barbry, *J. Biol. Chem.*, 269 (1994) 9921–9923.
[8] H. Tamura, K. Horike, H. Fukuda, T. Watanabe, *J. Biochem.* (*Tokyo*), 105 (1989) 299–306.
[9] V. Vignevich, D.M. Dooley, J.M. Guss, I. Harvey, M.A. McGuirl, H.C. Freeman, *J. Mol. Biol.*, 229 (1993) 243–245.
[10] J.H. Roh, H. Suzuki, H. Kumagai, M. Yamashita, H. Azakami, Y. Murooka, B. Mikami, *J. Mol. Biol.*, 238 (1994) 635–637.
[11] A. Rinaldi, P. Vecchini, G. Floris, *Prep. Biochem.*, 12 (1982) 11–28.
[12] H.G. Schwelberger, E. Bodner, *Biochim. Biophys. Acta*, 1340 (1997) 152–164.
[13] R.A. van der Meer, P.D. van Wassenaar, J.H. van Brouwershaven, J.A. Duine, *Biochem. Biophys. Res. Commun.*, 159 (1989) 726–733.
[14] D.I. Papac, A. Wong, A.J.S. Jones, *Anal. Chem.*, 68 (1996) 3215–3223.
[15] M.R. Hardy, R.R. Townsend, Y.C. Lee, *Anal. Biochem.*, 170 (1988) 54–62.
[16] A.K. Powell, D.J. Harvey, *Rapid Commun. Mass Spectrom.*, 10 (1996) 1027–1032.
[17] D.A. Dwek, *Chem. Rev.*, 96 (1996) 683–720.
[18] A.P. Corfield, M. Wember, R. Schauer, R. Rott, *Eur. J. Biochem.*, 124 (1982) 521–525.
[19] B. Kuster, T.J.P. Naven, D.J. Harvey, *J. Mass Spectrom.*, 31 (1996) 1131–1140.
[20] P. Chen, A.G. Baker, M.V. Novotny, *Anal. Biochem.*, 244 (1997) 144–151.
[21] A. Savitzky, M.J.E. Golay, *Anal. Chem.*, 36 (1964) 1627–1639.
[22] M. Stefansson, M.V. Novotny, *Carbohydr. Res.*, 258 (1994) 1–9.